Cell-Cell Affinity of Senescent Human Erythrocytes

Björn Neu, Samuel O. Sowemimo-Coker, and Herbert J. Meiselman
Department of Physiology and Biophysics, Keck School of Medicine, University of Southern California, Los Angeles, California 90033 USA

ABSTRACT During their 120-day life span, human red blood cells (RBC) undergo several physicochemical changes, including an increased tendency to aggregate in plasma or polymer solutions. This study was designed to examine potential associations between age-related differences in RBC mobility, aggregation, and membrane glycocalyx properties for cells suspended in buffer and in 3 g/dl solutions of 70.3 kDa dextran. A recent model for depletion-mediated RBC aggregation was employed to calculate the changes of glycocalyx properties that were consistent with experimental electrophoretic mobility (EPM) and aggregation data. Young and old cells were obtained by density separation, after which aggregation and EPM were determined versus ionic strength; old cells exhibited a two- to threefold greater aggregation in dextran. EPM of old cells was identical to young cells in polymer-free media yet was 4% greater in dextran. The greater EPM for old RBC indicates a larger polymer depletion layer, which could be explained either by a 10–15% decrease of their glycocalyx thickness or a similar percentage decrease of polymer penetration into their glycocalyx. The larger depletion layer leads to markedly elevated cell-cell affinities for old cells, with the computed affinity increases consistent with enhanced old RBC aggregation. These results provide a rational explanation for the aggregation and EPM behavior of old RBC, and raise the possibility of depletion-mediated interactions contributing to senescent cell removal from the circulation.

INTRODUCTION

The physicochemical changes associated with red blood cell (RBC) in vivo aging have been of interest for several decades, since understanding senescence of RBC should provide insight into cellular aging and the mechanism responsible for senescent cell clearance. Several reviews have summarized the ongoing work in the area of RBC aging and senescence (Berlin and Berk, 1975; Bratosin et al., 1998; Clark, 1988). Human RBC have a life span of ~120 days after which they are removed from the circulation (Berlin and Berk, 1975). The mechanisms responsible for clearance have not yet been fully defined, but are thought to relate, in part, to the appearance of age-associated receptors on the cell surface (Lutz, 1987; Tartakover-Matalon et al., 2000). Note that during in vivo aging there is an increase of cytoplasmic hemoglobin concentration and cell density (Linderkamp et al., 1983; Muller et al., 1992), and thus increased cell density corresponds to increased cell age (Berlin and Berk, 1975; Clark, 1988).

The effects of in vivo cell age on RBC-RBC interactions, and hence on their tendency to form reversible aggregates, have been previously studied. Nordt (1983) appears to be the first to report the effects of cell age on RBC aggregation, with several later investigations confirming his observations (Meiselman, 1993; Nash et al., 1987; Sowemimo-Coker et al., 1989; Whittingstall and Meiselman, 1991). In brief, it has been shown that when density-separated RBC are suspended in either autologous plasma or in various polymer solutions (e.g., dextran, polyvinylpyrrolidone), the denser cells exhibit significantly greater aggregation than the lighter cells. Efforts to date to provide a rational explanation for these age-associated differences in RBC aggregation have been unsuccessful: 1), reducing the volume of least-dense RBC to that of the densest cells only minimally affects aggregation, thus excluding an influence of cell size (Nash et al., 1987); 2), denser RBC are known to have increased levels of membrane-bound immunoglobulin G (Bratosin et al., 1998), yet nonenzymatic removal of immunoglobulin G does not alter the density-associated aggregation difference (Whittingstall and Meiselman, 1991); and 3), enzymatic treatment to remove membrane-associated sialic acid also fails to affect this difference (Nash et al., 1987).

The effects of cell age on RBC electrophoretic behavior have also been previously studied. Early reports indicated decreased electrophoretic mobility with increased density and hence with increased cell age (Yaari, 1969). Such findings were consistent with reduced electrostatic repulsion as an explanation for the increased RBC aggregation and the clearance of senescent RBC by phagocytosis. Later reports have failed to support these observations, and rather indicate no difference in the electrophoretic mobility of young and old human RBC when these cells are suspended in simple salt solutions (Luner et al., 1977; Meiselman et al., 1999; Seaman et al., 1977). However, mobility differences do exist for cells in either autologous plasma or in high molecular weight dextran solutions; denser human RBC exhibit significantly greater mobilities than less-dense cells in such media (Meiselman, 1993; Sowemimo-Coker et al., 1989; Walter and Widen, 1994).

This study was designed to examine potential associations between age-related differences in: 1), RBC electrophoretic

Submitted October 30, 2002, and accepted for publication February 27, 2003.

Address reprint requests to Dr. Björn Neu, Dept. of Physiology and Biophysics, Keck School of Medicine, 1333 San Pablo St., MMR 626, Los Angeles, CA 90033. Tel.: 323-442-1267; Fax: 323-442-1617; E-mail: neu@usc.edu.

Samuel O. Sowemimo-Coker's present address is Pall Life Sciences, Port Washington, NY.

0006-3495/03/07/75/10 $2.00

mobility; 2), RBC membrane glycocalyx physical properties; and 3), RBC aggregation due to a reduced polymer concentration near the surface of the cell (i.e., depletion-mediated RBC aggregation). In particular, we have employed our recently developed model for this type of red blood cell aggregation (Neu and Meiselman, 2002) in an effort to determine the changes of glycocalyx properties required to yield the observed electrophoretic mobilities and differences of aggregation.

MATERIAL AND METHODS

RBC preparation

Blood was obtained from the antecubital vein of healthy adult laboratory volunteers into heparin (5 IU/ml) and used within 4 h; the study was approved by the University of Southern California Institutional Review Board. Sodium chloride solutions having ionic strengths of 14.5 mM–145 mM were prepared using distilled water, with sorbitol added as appropriate to maintain isotonicity (Seaman, 1975). All solutions contained 0.3 mM sodium bicarbonate, with pH = 7.4 and osmolality = 295 ± 5 mOsm/kg. Portions of these solutions were then used to prepare media containing 3 g/dl dextran 70 (70.3 kDa, Pharmacia Fine Chemicals, Piscataway, NJ).

Red blood cells were density fractionated according to the method described by Murphy (1973). Whole blood was centrifuged at 2,000 × g for 10 min, the plasma removed and saved, and the buffy coat discarded. The RBC were resuspended at ~80% hematocrit in plasma, and then centrifuged in a fixed-angle rotor at 36,000 × g for 60 min at 30°C. At the end of this centrifugation, the top 10% of the packed cell column (termed young cells) and the bottom 10% (termed old cells) were separately harvested and washed twice in the appropriate medium. The cells were finally suspended at ~0.01% hematocrit for mobility studies or at 40 ± 1% hematocrit for aggregation measurements.

RBC electrophoretic mobility measurements

The electrophoretic mobility (EPM) in various media was measured at 25 ± 0.2°C using a cylindrical microelectrophoresis system (Model I, Rank Brothers, Cambridge, UK). This system was modified to allow the use of: 1), silver-silver chloride electrodes rather than solid platinum electrodes; and 2), sintered glass discs between the electrolyte in the electrode chambers and the RBC in the cylindrical sample chamber (Seaman, 1975). All RBC velocities were determined at the stationary level within the cylindrical sample chamber (i.e., at 0.239 R from the wall of the tube, where R is the tube radius of 0.134 cm). Measurements were carried out at a field strength of 3.5 volts/cm, with no evidence of electrical heating or related problems at this voltage; for suspending media of <0.0725 M ionic strength, 0.1 M KCl rather than 1 M KCl was used in the electrode chambers. Average EPM values were determined for at least 10 RBC per aliquot for three aliquots of each RBC suspension, with the field polarity reversed between each cell; the mean of the three separate EPM values was used for the suspension under study. For normal RBC in 0.145 M NaCl at pH = 7.4, this system yields an EPM of 1.096 ± 0.011 mm/sec/V/cm (mean ± SD, 26 donors).

RBC aggregation measurements

The extent of RBC aggregation was measured via an automated transparent cone-plate shearing instrument (Model MA-1 Aggregometer, Myrenne GmbH, Roetgen, Germany). This technique is based upon the increase of light transmission through a red blood cell suspension that occurs when individual RBC aggregate into rouleaux or rouleaux complexes. For this study, the Myrenne aggregometer was operated to provide the dimensionless aggregation index "M." This index is obtained by first shearing the RBC suspension in the gap between the rotating cone and fixed plate at 500 s^{-1} to disperse preexisting aggregates. The cone rotation is then abruptly stopped, and the light transmission through the suspension at stasis is integrated for 10 s; the final integrated value is displayed as the "M" index. This index increases with enhanced RBC aggregation and has been shown to correlate well with other measures of RBC aggregation (Rampling and Whittingstall, 1986; Schmid-Schönbein, 1996).

Miscellaneous techniques

Solution osmolalities were determined with a freezing point osmometer (Model 5004, Precision Systems, Natick, MA) and pH via a Radiometer model PHM71 system operating at 25°C (Radiometer A/S, Copenhagen, Denmark). Suspension hematocrits were determined using the microhematocrit method (12,000 × g, 4 min, IEC, Needham, MA). The viscosity of all solutions was measured, at 25°C, via a capillary viscometer (Viscometer II, Coulter Electronics, Luton, UK).

THEORY

Cell-cell affinities

We have recently proposed a theoretical model to evaluate depletion mediated RBC interactions in polymer solutions (Neu and Meiselman, 2002). In this model, the cell-cell interaction is given by the sum of attractive depletion interaction and repulsive electrostatic interaction; an overview of this approach is given below.

Depletion interaction

If a surface is in contact with a polymer solution and the loss of configurational entropy of the polymer is not balanced by adsorption energy, a depletion layer develops near the surface. Within this layer, the polymer concentration is lower than in the bulk phase. Thus, as two RBC approach, the difference of solvent chemical potential (i.e., the osmotic pressure difference) between the intercellular polymer-poor depletion zone and the bulk phase results in solvent displacement into the bulk phase and hence depletion interaction. Due to this interaction, an attractive force develops that tends to minimize the polymer-reduced space between the cells and thus promotes aggregation (Fleer et al., 1993).

Examination of the energetics of depletion layers requires distinguishing between so-called "hard" and "soft or hairy" surfaces. Hard surfaces are considered to be smooth and do not allow polymer penetration into the surface, whereas soft surfaces, such as the RBC glycocalyx, are characterized by a layer of attached macromolecules that can be penetrated in part or entirely by the free polymer in solution (Fleer et al., 1993; Vincent et al., 1986). For two adjacent cells with soft surfaces at a separation distance d, a glycocalyx thickness δ, a depletion layer thickness Δ, and a penetration p of the polymers into the glycocalyx, the depletion interaction energy w_D is given by (Neu and Meiselman, 2002)

$$w_D = -2\Pi\left(\Delta - \frac{d}{2} + \delta - p\right) \quad (1)$$

for $(d/2 - \delta + p) \leq \Delta$ and is zero for $(d/2 - \delta + p) > \Delta$. The osmotic pressure term Π is calculated using a virial equation neglecting all coefficients higher than the second (B_2):

$$\Pi = \frac{RT}{M_2} c_2^b + B_2 (c_2^b)^2, \quad (2)$$

where R, T, and M_2 are the gas constant, absolute temperature, and the molecular weight of the polymer, and c_2^b represents the bulk polymer concentration.

An approach introduced by Vincent (1990) is used to calculate the dependence of the depletion layer thickness (Δ) on the properties of the polymer:

$$\Delta = -\frac{1}{2}\frac{\Pi}{D} + \frac{1}{2}\sqrt{\left(\frac{\Pi}{D}\right)^2 + 4\Delta_0^2}. \quad (3)$$

The parameter D is a function of the bulk polymer concentration (c_2^b):

$$D = \frac{2k_B T}{\Delta_0^2}\left(\frac{c_2^b N_a}{M_2}\right)^{2/3}, \quad (4)$$

where k_B and N_a are the Boltzmann constant and Avogadro's number. Δ_0 is the depletion thickness for vanishing polymer concentration and is equal to $1.4 \cdot R_g$, where R_g is the polymer's radius of gyration (Vincent, 1990).

Intuitively, the penetration depth p of the free polymer into the attached layer should depend on the polymer type, concentration and molecular size, and would be expected to be larger for small molecules and to increase with increasing polymer concentration due to increasing osmotic pressure. One possibility is to calculate p by assuming that penetration proceeds until the local osmotic pressure developed in the attached layer is balanced by the osmotic pressure of the bulk solution (Vincent et al., 1986). It is also possible to consider that the attached polymers collapse under the osmotic pressure of the bulk polymer (Jones and Vincent, 1989). However, it is difficult to accurately apply such a model to RBC in polymer or protein solutions since too little is known about the physicochemical properties of the glycocalyx, and in particular, about the interaction between the glycocalyx and different polymers or proteins. An exponential approach is thus used for describing polymer penetration into the glycocalyx (Neu and Meiselman, 2002):

$$p = \delta\left(1 - e^{-c_2^b/c_2^p}\right), \quad (5)$$

where c_2^p is the penetration constant of the polymer (i.e., when c_2^p equals c_2^b, p is 63% of δ). In this approach, δ is assumed to be independent of bulk polymer concentration, and therefore p is essentially a linear function of c_2^b at low concentrations (relative to c_2^p) and asymptotically approaches δ at high concentrations.

Electrostatic interaction

The electrostatic free energy of two cells can be calculated by considering an isothermal charging process:

$$E = \frac{1}{2}\int_0^d \int_0^\rho \psi(\rho, x) d\rho\, dx, \quad (6)$$

where ψ is the electrostatic potential between the cells as a function of the charge density (ρ). To calculate the electrostatic interaction energy w_E between two cells, one first calculates the free energy of the two cells at a separation distance d, then deducts the free energy of two single cells (i.e., as $d \to \infty$). To calculate the electrostatic potential ψ for RBC, it is necessary to solve the Poisson-Boltzmann equation. The linear approximation that is usually suitable for moderate electric potentials is employed herein (Donath et al., 1993). In this case the electrostatic potential between two cells or for a single cell for $d \to \infty$ reads as follows (Donath et al., 1993):

$$\Psi(x) = \frac{1}{\kappa\varepsilon\varepsilon_o}\left[\frac{\cosh(\kappa x)}{\sinh(\kappa d)}\int_0^d \rho(\xi)\cosh(\kappa(d-\xi))d\xi - \int_0^x \rho(\xi)\sinh(\kappa(x-\xi))d\xi\right], \quad (7)$$

where ε, ε_o, and κ are the relative and absolute permitivities and the inverse of the Debye-Hückel length, respectively. Considering the charges to be uniformly distributed within the glycocalyx, the charge density (ρ) for $x \leq \delta$ is:

$$\rho(x) = \frac{\sigma}{\delta}, \quad (8)$$

and for $x > \delta$ the charge density is equal to zero, where σ is the surface charge density (i.e., charge per surface area). Finally, the total interaction energy (w_T) is given by the sum of the electrostatic interaction energy (w_E) and the depletion interaction energy (w_D) (Neu and Meiselman, 2002).

Electrophoretic mobility

If a particle is assumed to be at rest, its electrophoretic mobility is usually considered to be equal to the electroosmotic slip velocity $u_e(\infty)$ far from its surface. To obtain the electroosmotic slip velocity, one has to solve the appropriate Navier-Stokes equation with the impressed field E as the driving force. However, it is more convenient to consider an alternative approach: the problem of a pressure gradient-driven streaming current along a flat surface. Both approaches are equivalent (Donath and Voigt, 1986), but the latter allows separate calculations for the hydrodynamic and electrostatic portions. In this case, the perpendicular velocity profile $u_0(x)$ of a pressure gradient driven flow along a hairy surface of thickness δ, which has a constant friction factor a, becomes (Donath et al., 1993):

$$u_0(x) = \begin{cases} \dfrac{\sinh(ax)}{\eta_s a \cosh(a\delta)} & x < \delta \\ \dfrac{x-\delta}{\eta_s} + \dfrac{\tanh(a\delta)}{\eta_s a} & x \geq \delta \end{cases}. \quad (9)$$

Note that the bulk viscosity η_s and the viscosity inside the glycocalyx are assumed to be the same, that the physical meaning of a is the inverse of the flow penetration depth, and that a depends on the hydrodynamic friction and the viscosity (Donath et al., 1996; Levine et al., 1983).

The perpendicular profile $u_p(x)$ of a pressure gradient-driven flow along a hairy surface with a polymer depletion layer is (Donath et al., 1997):

$$u_p(x) = \begin{cases} \dfrac{\sinh(a_p x)}{\eta_s a \cosh(a_p \delta)} & x < \delta \\ \displaystyle\int_\delta^x \frac{1}{\eta(\xi)} d\xi + \frac{\tanh(a_p\delta)}{\eta_s a_p} & x \geq \delta \end{cases}. \quad (10)$$

In this case it is necessary to consider the viscosity profile $\eta(x)$ and an increased value for the friction factor inside the glycocalyx (a_p) due to immobilized polymer. The effective Stokes friction f of the immobilized polymer is characterized by the volume density N_v and the hydrodynamic radius of the dextran monomer segments, r_{seg} (Levine et al., 1983):

$$f = 6\pi N_v \eta_s r_{seg}, \quad (11)$$

where N_v is given by the segment molecular weight and the polymer concentration within the glycocalyx (see Results), and for dextran r_{seg} is taken as 6.5 Å (Evans and Needham, 1988). Assuming that the intrinsic friction (a) and thickness of the charged layer (i.e., glycocalyx) are not affected by the presence of the immobilized polymer, a_p of the charged layer plus the immobilized polymer is given by (Neu et al., 2001):

$$a_p^2 = a^2 + \frac{f}{\eta_s}. \quad (12)$$

Thus, given an appropriate viscosity profile (i.e., concentration profile) and the electrostatic potential (Eqs. 7 and 8), it is possible to generate an expression for the ratio of the mobility of particles in a polymer-free solution b_0 and in a solution containing polymer b_p (Donath et al., 1993; Donath and Voigt, 1986):

$$\frac{b_0}{b_p} = \frac{\int_0^\infty u_0(\xi)\Psi(\xi)d\xi}{\int_0^\infty u_p(\xi)\Psi(\xi)d\xi}. \quad (13)$$

RESULTS

Experimental results

Aggregation behavior of young and old RBC in 3 g/dl dextran 70, as a function of suspending medium ionic strength and hence as a function of Debye-Hückel length, is shown in Fig. 1. Note that the Debye-Hückel length is inversely related to ionic strength and thus increases with decreasing strength; at an ionic strength of 145 mM, the Debye-Hückel length is 0.79 nm. The figure clearly indicates that aggregation of old cells is much greater than that of young cells. At normal ionic strength (i.e., 145 mM), the old/young ratio is 3.26 (i.e., 226% greater for old cells) and over a Debye-Hückel length range of 0.79–1.13 nm, this ratio remains essentially unaltered (mean ± SD = 3.16 ± 0.09, $p < 0.001$). The ratio decreases slightly to 2.32 at 1.78 nm, yet is still markedly greater than unity. At the lowest ionic strength (2.5 nm), neither young nor old RBC exhibits aggregation in 3 g/dl dextran 70.

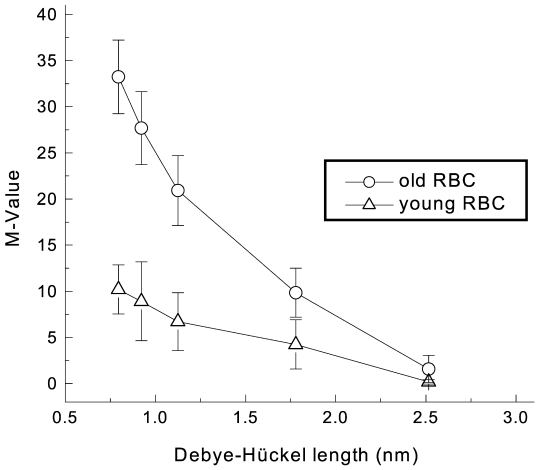

FIGURE 1 Experimental values of RBC aggregation versus Debye-Hückel length for age-separated cells suspended in 3 g/dl solutions of 70.3 kDa dextran; all solutions were made isotonic by addition of sorbitol. Over the range of 0.79–1.78 nm, the old/young aggregation ratio was 2.95 ± 0.43 (mean ± SD, $p < 0.001$).

Electrophoretic mobilities of young and old RBC, as a function of ionic strength, are shown in Fig. 2 *A* for cells in dextran-free media and in Fig. 2 *B* for cells in media containing 3 g/dl dextran 70. For cells in polymer-free solutions (Fig. 2 *A*), the effects of ionic strength on EPM behavior are consistent with earlier reports (Bäumler et al., 1996): the mean mobility at an ionic strength of 145 mM is 1.09 μm/sec/v/cm and increases to 2.65 at 14.5 mM. Most notable in Fig. 2 *A* is that the mean ratio of old/young EPM does not differ significantly from unity over the entire range of Debye-Hückel lengths (mean ± SD = 1.010 ± 0.007, $p > 0.2$).

In contrast to the findings presented in Fig. 2 *A*, age-separated RBC in 3 g/dl dextran 70 do exhibit an old/young EPM mobility ratio greater than unity: over the Debye-Hückel lengths shown, the ratio is 1.042 ± 0.012 (mean ± SD, $p < 0.005$) and is not a function of ionic strength. Thus, old RBC in the dextran media have a significant, ~4% greater EPM than young cells, whereas no such difference is observed for these cells in dextran-free media. The EPM data in Fig. 2, *A* and *B*, also indicate that the magnitude of the EPM decrease for both young and old cells in the dextran media is markedly less than predicted based upon measured

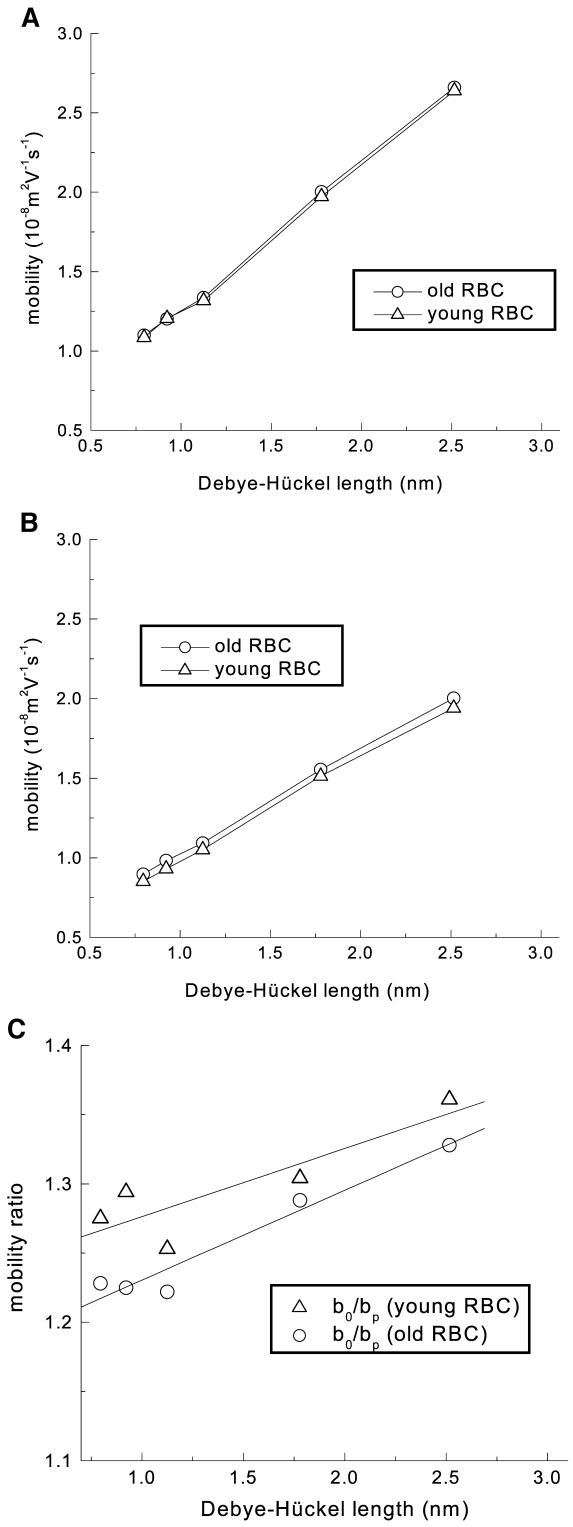

FIGURE 2 Experimental values of RBC electrophoretic mobility (EPM) versus Debye-Hückel length for age-separated cells in isotonic media; all solutions were made isotonic by addition of sorbitol. No significant differences were found for cells in dextran-free media (panel *A*). However, old RBC had a higher EPM in 3 g/l solutions of 70.3 kDa dextran (panel *B*); mean old/young ratio over the Debye-Hückel lengths shown was 1.042 ± 0.012 (mean ± SD, $p < 0.005$). Ratios of EPM for cells in dextran-free media (b_o) divided by cells in dextran (b_p) in panel *C* indicate greater polymer depletion near surface of old RBC (see text).

bulk phase viscosities. For example, at an ionic strength of 145 mM, the viscosity of the dextran medium is 93% greater than the dextran-free medium (1.70 vs. 0.88 mPa · s), yet the decrease of EPM is only 19% (old cells) to 22% (young cells).

These viscosity-related EPM results strongly imply polymer depletion near the RBC surface and hence reduced local viscosities near the cell. For Debye-Hückel lengths less than the depletion layer, this local viscosity rather than bulk viscosity is a determinant of cell mobility (Bäumler et al., 1996). Fig. 2 *C* presents a graphical confirmation of this depletion effect (i.e., media viscosity ratio with and without dextran is 1.95 yet cell mobility ratios are much less at all Debye-Hückel lengths). Note also that the extrapolated mobility ratio intercept is greater for the old cells, thus indicating a lower effective viscosity near the surface of these cells (Eq. 11).

Theoretical results

Initial considerations

Given the more than threefold greater aggregation for older cells (Fig. 1) yet the very modest but significant increase of EPM for these cells in the dextran media (Fig. 2 *B*), it is important to resolve the following question: are the differences in polymer depletion suggested by Fig. 2 sufficient to explain differences in cell-cell affinity and thus the differences in young versus old RBC aggregation? It is notable that the equal mobilities of age-separated cells in polymer-free media (Fig. 2 *A*) do not necessarily imply that they have the same surface charge density, since cellular EPM is determined by surface charge density, glycocalyx thickness, and hydrodynamic friction (Donath and Voigt, 1986). Thus, for example, it is possible that changes of surface charge density are accompanied by differences in glycocalyx thickness leading to little or no changes of mobility (see below).

The greater EPM in dextran media for old RBC (Fig. 2 *B*), and hence the larger depletion effect for these cells, suggests two possible causes related to either differences of glycocalyx thickness or to differences of glycocalyx penetration by the polymer (Fig. 3). One possibility might be that the glycocalyx thickness of old cells (δ_o) is thinner compared to the thickness of young cells (δ_y). This decrease of thickness would move the shear plane closer to the cell surface leading to a reduced viscosity outside the glycocalyx and a reduced hydrodynamic friction within the glycocalyx, and thus a higher mobility. Another possibility might be decreased polymer penetration for old cells (p_o) compared to young cells (p_y), perhaps due to altered glycocalyx density or

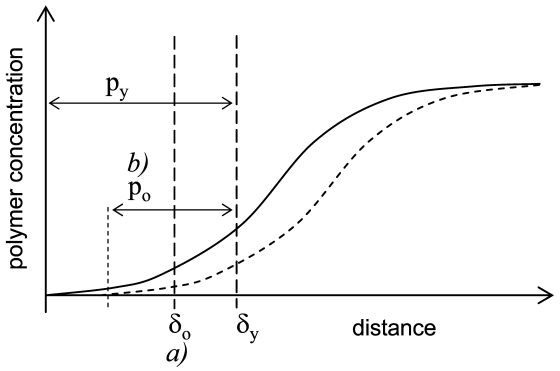

FIGURE 3 Schematic representation of two possible causes for a greater polymer depletion effect for old RBC: *a*) Thinner glycocalyx for old cells, in which the polymer concentration profile (*solid curved line*) is the same for both young and old cells but the glycocalyx thickness for old cells (δ_o) is less than for young cells (δ_y); *b*) Decreased polymer penetration of the glycocalyx, in which the penetration for old cells (p_o) is less than for young cells (p_y), and thus the polymer concentration profiles differ (young, *solid curved line*; old, *dashed curved line*). Both causes yield a reduced viscosity in the Debye atmosphere and thus a higher electrophoretic mobility for old RBC.

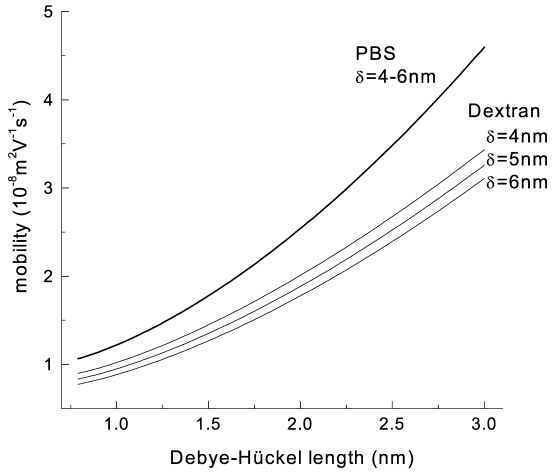

FIGURE 4 Calculated effects of ±20% variations of cell glycocalyx thickness on RBC electrophoretic mobility (EPM), as a function of Debye-Hückel length, for cells in dextran-free media (*upper curve marked PBS*) and in 3 g/dl *solutions* of 70.3 kDa dextran (*lower curves*). No effects on EPM were noted for the dextran-free media whereas ±20% thickness changes for cells in dextran result in reciprocal ±7% changes of EPM.

polymer-glycocalyx affinity. Again, this would lead to a reduced viscosity outside the glycocalyx and a reduced hydrodynamic friction within the glycocalyx, and thus higher mobilities of the older cells in polymer solutions.

Glycocalyx thickness effects

Considering first cells in polymer-free media, the calculated effects of variations of glycocalyx thickness (δ) on surface charge density (σ) are shown in the upper portion of Table 1 for RBC at an ionic strength of 145 mM. These calculated values are constrained by the requirement that the resulting EPM values in polymer-free medium remain unaltered; assumed values for an average red blood cell are a glycocalyx thickness of 5 nm, a surface charge density of 0.036 C/m^2, and a friction factor a of 1.09 nm^{-1} (Bäumler et al., 1996; Donath et al., 1996). In this case of unaltered electrophoretic mobility, glycocalyx thickness and computed surface charge density have parallel and nearly identical changes (e.g., for a 20% decrease of δ from 5 to 4 nm, σ decreases by 19%). Fig. 4 (*upper curve*) presents the effects of ionic strength on EPM as a function of glycocalyx thickness: for cells in polymer-free media, EPM shows the expected increase with Debye-Hückel length (Fig. 2 *A*) but is insensitive to changes of glycocalyx thickness.

TABLE 1 Calculated effects of glycocalyx thickness on RBC charge and cell-cell affinity

δ (nm)	4.0	4.5	5.0	5.5	6.0
σ (C/m^2)	0.029	0.033	0.036	0.040	0.043
$w_{3\%}$ (μJ/m^2)	−8.9	−6.3	−3.8	−1.2	–
w_{max} (μJ/m^2)	−9.7	−6.6	−4.6	−3.2	−2.4

Calculated σ values are for cells in polymer-free PBS, $w_{3\%}$ are for cells in 3 g/dl dextran 70 kDa, and w_{max} are the maximum cell-cell affinities for cells in 70 kDa dextran (Fig. 7). All values are for RBC in 145 mM ionic strength media using a glycocalyx friction factor a = 1.09 nm^{-1}.

The calculated surface charge density values in Table 1 now allow evaluation of expected RBC mobilities in solutions containing 3 g/dl dextran. Since the polymer concentration is relatively high, it is possible to assume complete penetration with $p = \delta$ (Neu and Meiselman, 2002). Further, the concentration profile of a nonadsorbing polymer is approximated by (de Gennes, 1979):

$$c_2(x) = c_2^{\mathrm{b}} \tanh^2\left(\frac{x}{\Delta}\right), \tag{14}$$

where c_2^{b} is the bulk polymer concentration and Δ is given by Eq. 3. At each glycocalyx thickness, it is assumed that the resulting value of polymer concentration at the glycocalyx edge remains constant throughout the glycocalyx, and thus the thickness of the glycocalyx determines the polymer concentration within the glycocalyx.

The Huggins expression was used for estimating solution viscosity (η) based upon polymer concentration (Flory, 1953):

$$\eta = \eta_0(1 + [\eta]c_2 + k'[\eta]^2 c_2^2), \tag{15}$$

where η_0 is the viscosity of the solvent, which varies with ionic strength due to the changing sorbitol content (i.e., 0.88 mPa·s for 145 mM and 0.97 mPa·s for 14.5 mM); $[\eta]$ is the intrinsic viscosity of the 70.3 kDa dextran ($[\eta] = 0.23$ dl/g); and k' a polymer dependent constant ($k' = 0.48$).

Fig. 4 (*lower curves*) presents calculated absolute values of RBC mobility as a function of glycocalyx thickness for cells in 3 g/dl dextran, and Fig. 5 shows these calculated mobility values relative to those for cells having a 5 nm thick glycocalyx. These results indicate the reciprocal relationship

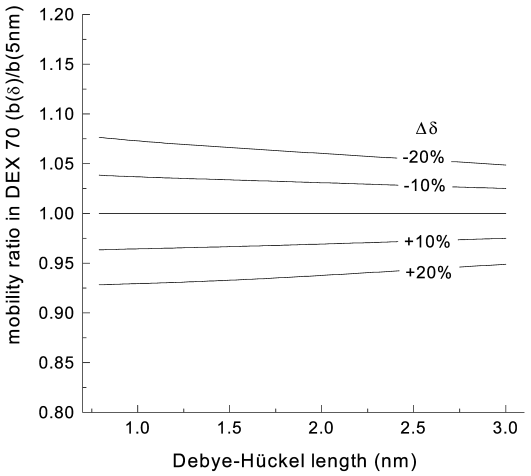

FIGURE 5 Calculated effects of ±20% variations of cell glycocalyx thickness on electrophoretic mobility (EPM), as a function of Debye-Hückel length, for cells in 3 g/dl solutions of 70.3 kDa dextran. EPM data are shown relative to EPM values for a glycocalyx thickness of 5 nm (i.e., $b(\delta)/b(5\text{ nm})$), and thus the mobility ratio is 1.0 for an unaltered 5 nm thick glycocalyx.

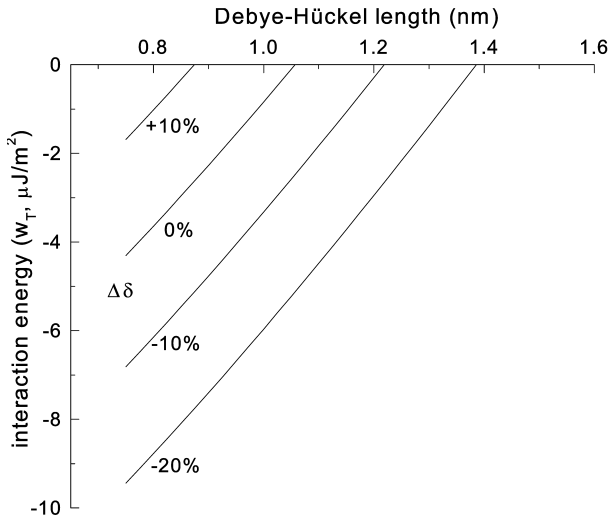

FIGURE 6 Calculated effects of variations of glycocalyx thickness on cell-cell affinity (w_T), as a function of Debye-Hückel length, for cells in 3 g/dl solutions of 70.3 kDa dextran. Complete polymer penetration of the glycocalyx (i.e., $p = \delta$) was assumed.

between glycocalyx thickness and RBC mobility: 10% and 20% increases of thickness reduce the EPM by ~3% and 7%, respectively, whereas the same decreases of thickness raise EPM values by ~3% and 7%. Thus a 10–20% decrease of old cell glycocalyx thickness is consistent with the 4.2% greater EPM for these cells (Fig. 2 *B*).

Finally, it is possible to use the glycocalyx thickness and calculated surface charge density shown in Table 1 to predict expected cell-cell affinity (w_T) for cells in dextran-containing media. Two situations were considered: 1), effects of ionic strength and glycocalyx thickness with complete penetration of the glycocalyx (i.e., $p = \delta$) at a constant dextran concentration of 3 g/dl (Fig. 6); and 2), effects of dextran concentration and glycocalyx thickness with a penetration constant (c_2^p) of 0.7 g/dl (Neu and Meiselman, 2002) and a constant ionic strength of 145 mM (Fig. 7). Both Figs. 6 and 7 lead to the same observation: slight changes of glycocalyx thickness lead to multifold changes of cell-cell affinity, yet these changes of thickness are associated with only minor changes of cell mobility. Specifically, at 3 g/dl dextran as employed herein and at 145 mM ionic strength, a 10% decrease of thickness (i.e., 5–4.5 nm) results in a 60% increase of cell-cell affinity but only an ~3% increase of RBC mobility (Figs. 5–7).

Glycocalyx penetration effects

An alternative approach is to evaluate the possibility of changes in polymer penetration of the glycocalyx with an unaltered glycocalyx thickness. Calculated results for the effects of decreased polymer penetration (not shown) lead to essentially the same results as those observed for decreased glycocalyx thickness (Figs. 6 and 7). For example, for RBC with a 5 nm thick glycocalyx in 3 g/dl dextran 70 kDa at 145 mM ionic strength, a 20% decrease of polymer penetration (i.e., from 5 to 4 nm) yields about the same increases of mobility and surface affinity as calculated above for complete penetration and a 5–4 nm decrease in glycocalyx thickness. Thus, relatively modest decreases of glycocalyx thickness or of polymer penetration yield EPM and cell-cell affinity changes that are appropriate for old red blood cells.

DISCUSSION

Although the general phenomenon of red blood cell aggregation has been studied for decades (Chien, 1975;

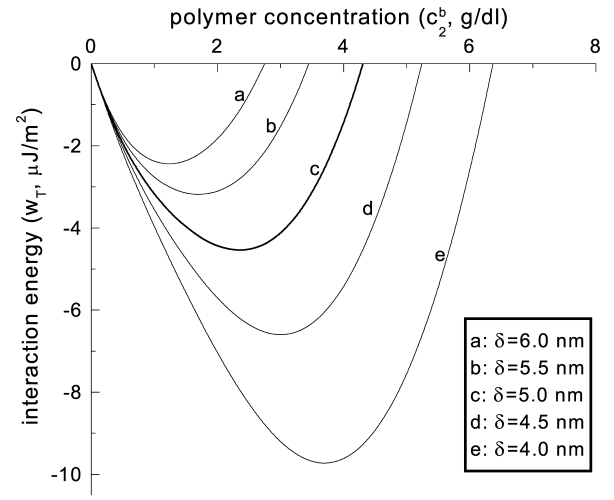

FIGURE 7 Calculated effects of ±20% variations of glycocalyx thickness on cell-cell affinity (w_T) for cells in media containing various concentrations of 70.3 kDa dextran. Media ionic strength was held constant at 145 mM and a penetration constant (c_2^p) of 0.7 g/dl was assumed.

Lowe, 1988; Schmid-Schönbein, 1996), the effects of RBC cellular factors on RBC ''aggregability'' (i.e., the aggregation tendency of red blood cells when resuspended in a defined macromolecular solution) have only more recently received attention. Abnormalities of various mechanical characteristics, such as membrane rigidity, membrane viscosity, and cytoplasmic viscosity, have been demonstrated to reduce the rate and extent of aggregation (Meiselman, 1993; Nash et al., 1987; Sowemimo-Coker et al., 1989). Marked changes of RBC shape from the normal biconcave form, as well as decreased cellular deformability, also lead to decreased aggregation (Meiselman, 1993). Although it is possible to postulate causal relations between altered cell mechanical behavior and altered tendency to aggregate, mechanisms responsible for age-specific effects in red blood cell aggregation have remained obscure.

The results of this study provide insight into mechanisms responsible for the greatly enhanced aggregation tendency of denser, older human erythrocytes. Based upon established particle electrophoretic theory (Donath et al., 1996; Levine et al., 1983) and a recently developed depletion model for polymer-induced RBC aggregation (Neu and Meiselman, 2002), we have focused on the effects of small changes of polymer depletion on RBC mobility and RBC-RBC affinity. The calculated results for glycocalyx thickness are consistent with our experimental findings: 1), equal mobilities for young and old cells in polymer-free media (Figs. 2 *A* and 4); 2), small decreases of thickness yield slightly greater mobilities for cells suspended in media containing 3 g/dl dextran (Figs. 2 *B*, 4, and 5); and 3), the same small decreases of thickness result in markedly increased cell-cell affinity for cells in the 3 g/dl dextran media (Figs. 6 and 7). Similar computed results (i.e., greater mobility and cell-cell affinity in dextran) occur by assuming constant surface charge density and constant glycocalyx thickness, then decreasing the penetration depth. Since the goal of this study was to calculate surface affinities consistent with EPM data, such an observation does not vitiate our findings: differences of depletion layer thickness were of interest rather than a single mechanism responsible for such differences.

The increase of cell-cell affinity cited above is of critical importance, since increased cell-cell affinity results in increased RBC aggregation (Buxbaum et al., 1982; Chien, 1975; Neu and Meiselman, 2002). Using the same Myrenne aggregometer system as employed herein, Nash and co-workers (Nash et al., 1987) have presented aggregation-polymer concentration data for unfractionated human RBC suspended in 145 mM solutions of 70 kDa dextran. Their results indicate an ~2.4-fold increase of aggregation as the polymer concentration is increased from 1.5 to 3.0 g/dl. For the same molecular weight dextran and the same concentration increase, Buxbaum et al. (1982) indicate an ~70% increase of RBC-RBC affinity. Our calculated results also indicate an ~70% increase of RBC-RBC affinity as the glycocalyx thickness is decreased from 5 to 4.5 nm (Fig. 7, 3 g/dl). Thus our computed findings appear to be in qualitative and quantitative agreement with observed aggregation differences between young and old cells. Small increases in polymer depletion, which might be due to small decreases of glycocalyx thickness or of polymer penetration or both during in vivo aging, could therefore easily explain the greatly enhanced aggregation tendency of older red blood cells (Figs. 1, 6, and 7).

With regard to the agreement between the computed results from our model and experimental findings, some additional comments seem appropriate:

1. For all ionic strengths where RBC aggregation was observed (Fig. 1), the Debye-Hückel length is always smaller than the 4–6 nm range of glycocalyx thickness used for computing EPM and cell-cell affinity. Thus, with a constant charge density ρ, a decrease of glycocalyx thickness as suggested as a possibility for old RBC only slightly alters the electrostatic potential between adjacent RBC and thus minimally affects electrostatic repulsive forces. The calculated increase in cell-cell affinity is therefore almost exclusively due to increased depletion-mediated forces resulting from the decreased glycocalyx thickness (Figs. 3 and 6).
2. Numerous structural changes of the RBC glycocalyx are known to occur during in vivo aging (Bratosin et al., 1998; Clark, 1988), and several studies have addressed negative surface charge versus cell age. The main source of RBC negative surface is the carboxyl group of membrane-bound *N*-acetylneuramic acid (Seaman, 1975). Even though most reports favor age-dependent desialylation, some link the loss of sialic acid to loss of membrane surface area, thereby implying no change in sialic acid content per surface area (Luner et al., 1977; Lutz and Fehr, 1979; Seaman et al., 1977). However, in addition to confirming the decrease of sialic acid for older cells, Bratosin and co-workers (Bratosin et al., 1998) indicate that the decrease is due to enzymatic activity as well as to reduced surface area. Consequently, because of this enzymatic process, loss of charges per membrane surface area seems probable. Since EPM in polymer-free media is the same for young and old cells (Fig. 2 *A*), and since equal EPM in polymer-free media indicates equal charge density ρ, our assumption of a thinner glycocalyx yielding an unaltered charge density for old RBC seems reasonable.

Finally, it is of interest to consider whether age-associated changes of RBC surface affinity plays a role in the recognition and eventual elimination of senescent cells from the circulation. Most reports favor an age-dependent expression of an antigenic site that is recognized by macrophages within the reticuloendothelial system and which leads to macrophage engulfment and destruction of senescent RBC (Beutler et al., 1995; Clark, 1988; Tartakover-Matalon et al., 2000). Additionally, older, more-dense erythrocytes

have been shown to have increased membrane viscosity and hence a longer time constant for viscoelastic shape change (Nash and Meiselman, 1983); such altered rheologic behavior could lead to slower deformation and thus longer residence times within macrophage-lined regions of splenic, hepatic, and bone marrow sinusoids. However, recognition as well as eventual entrapment of effete RBC by macrophages requires close proximity between erythrocyte and macrophage membranes (Beutler et al., 1995), and thus depletion-mediated forces could aid in achieving the required cell-cell separation. Although such forces would be expected to promote receptor-ligand mediated interactions via bringing these molecular species into appropriate proximity, the specific effects of such forces and of the relative dimensions of the receptors, the depletion layer and the glycocalyx are currently unknown and thus warrant additional research activity.

The authors express their appreciation to Ms. Rosalinda B. Wenby for technical assistance.

This work was supported by National Institutes of Health grants HL 15722 and HL 48484.

REFERENCES

Bäumler, H., E. Donath, A. Krabi, W. Knippel, A. Budde, and H. Kiesewetter. 1996. Electrophoresis of human red blood cells and platelets. Evidence for depletion of dextran. *Biorheology.* 33:333–351.

Berlin, N. I., and P. D. Berk. 1975. The biological life of the red cell. *In* The Red Blood Cell. D.M. Surgenor, editor. Academic Press, New York. 957–1019.

Beutler, E., M. A. Lichtman, B. S. Coller, and T. J. Kipps. 1995. Hematology. McGraw-Hill, New York.

Bratosin, D., J. Mazurier, J. P. Tissier, J. Estaquier, J. J. Huart, J. C. Ameisen, D. Aminoff, and J. Montreuil. 1998. Cellular and molecular mechanisms of senescent erythrocyte phagocytosis by macrophages. A review. *Biochimie.* 80:173–195.

Buxbaum, K., E. Evans, and D. E. Brooks. 1982. Quantitation of surface affinities of red blood cells in dextran solutions and plasma. *Biochemistry.* 21:3235–3239.

Chien, S. 1975. Biophysical behavior of red cells in suspensions. *In* The Red Blood Cell. D.M. Surgenor, editor. Academic Press, New York. 1031–1133.

Clark, M. R. 1988. Senescence of red blood cells: progress and problems. *Physiol. Rev.* 68:503–554.

de Gennes, P.-G. 1979. Scaling Concepts in Polymer Physics. Cornell University Press, Ithaca, N.Y.

Donath, E., A. Budde, E. Knippel, and H. Bäumler. 1996. ''Hairy surface layer'' concept of electrophoresis combined with local fixed surface charge density isotherms: Application to human erythrocyte electrophoretic fingerprinting. *Langmuir.* 12:4832–4839.

Donath, E., P. Kuzmin, A. Krabi, and A. Voigt. 1993. Electrokinetics of structured interfaces with polymer depletion—a theoretical study. *Colloid Polym. Sci.* 271:930–939.

Donath, E., and A. Voigt. 1986. Streaming current and streaming potential on structured surfaces. *J. Colloid Interface Sci.* 109:122–139.

Donath, E., D. Walther, V. N. Shilov, E. Knippel, A. Budde, K. Lowack, C. A. Helm, and H. Möhwald. 1997. Nonlinear hairy layer theory of electrophoretic fingerprinting applied to consecutive layer by layer polyelectrolyte adsorption onto charged polystyrene latex particles. *Langmuir.* 13:5294–5305.

Evans, E., and D. Needham. 1988. Attraction between lipid bilayer membranes in concentrated solutions of nonadsorbing polymers—comparison of mean-field theory with measurements of adhesion energy. *Macromolecules.* 21:1822–1831.

Fleer, G. J., M. A. Cohen Stuart, J. H. M. H. Scheutjens, T. Cosgrove, and B. Vincent. 1993. Polymers at Interfaces. Chapman & Hall, London.

Flory, P. J. 1953. Principles of Polymer Chemistry. Cornell University Press, Ithaca, New York.

Jones, A., and B. Vincent. 1989. Depletion flocculation in dispersions of sterically stabilized particles. 2. Modifications to theory and further studies. *Colloids and Surfaces.* 42:113–138.

Levine, S., M. Levine, K. A. Sharp, and D. E. Brooks. 1983. Theory of the electrokinetic behavior of human erythrocytes. *Biophys. J.* 42:127–135.

Linderkamp, O., P. Y. Wu, and H. J. Meiselman. 1983. Geometry of neonatal and adult red blood cells. *Pediatr. Res.* 17:250–253.

Lowe, G. D. O. 1988. Clinical Blood Rheology. CRC Press, Boca Raton, FL.

Luner, S. J., D. Szklarek, R. J. Knox, G. V. F. Seaman, J. Y. Josefowicz, and B. R. Ware. 1977. Red cell charge is not a function of cell age. *Nature.* 269:719–721.

Lutz, H. U. 1987. Red cell clearance (a review). *Biomed. Biochim. Acta.* 46:S65–S71.

Lutz, H. U., and J. Fehr. 1979. Total sialic acid content of glycophorins during senescence of human red blood cells. *J. Biol. Chem.* 254:11177–11180.

Meiselman, H. J. 1993. Red-blood-cell role in RBC aggregation. *Clin. Hemorheol. Microcirc.* 13:575–592.

Meiselman, H. J., O. K. Baskurt, S. O. Sowemimo-Coker, and R. B. Wenby. 1999. Cell electrophoresis studies relevant to red blood cell aggregation. *Biorheology.* 36:427–432.

Muller, G. H., H. Schmid-Schonbein, and H. J. Meiselman. 1992. Development of viscoelasticity in heated hemoglobin solutions. *Biorheology.* 29:203–216.

Murphy, J. R. 1973. Influence of temperature and method of centrifugation on the separation of erythrocytes. *J. Lab. Clin. Med.* 82:334–341.

Nash, G. B., and H. J. Meiselman. 1983. Red cell and ghost viscoelasticity. Effects of hemoglobin concentration and in vivo aging. *Biophys. J.* 43:63–73.

Nash, G. B., R. B. Wenby, S. O. Sowemimo-Coker, and H. J. Meiselman. 1987. Influence of cellular properties on red cell aggregation. *Clin. Hemorheol. Microcirc.* 7:93–108.

Neu, B., J. K. Armstrong, T. C. Fisher, H. Bäumler, and H. J. Meiselman. 2001. Electrophoretic mobility of human red blood cells coated with poly(ethylene)glycol. *Biorheology.* 38:389–403.

Neu, B., and H. J. Meiselman. 2002. Depletion-mediated red blood cell aggregation in polymer solutions. *Biophys. J.* 83:2482–2490.

Nordt, F. J. 1983. Hemorheology in cerebrovascular diseases: approaches to drug development. *Ann. N. Y. Acad. Sci.* 416:651–661.

Rampling, M. W., and P. Whittingstall. 1986. A comparison of five methods for estimating red cell aggregation. *Klin. Wochenschr.* 64:1084–1088.

Schmid-Schönbein, H. 1996. Hemorheology. *In* Comprehensive Human Physiology. R. Greger and U. Windkorst, editors. Springer-Verlag, Berlin. 1747–1792.

Seaman, G. V. F. 1975. Electrokinetic behavior of red cells. *In* The Red Blood Cell. D.M. Surgenor, editor. Academic Press, New York. 1135–1229.

Seaman, G. V. F., R. J. Knox, F. J. Nordt, and D. H. Regan. 1977. Red cell aging. I. Surface charge density and sialic acid content of density-fractionated human erythrocytes. *Blood.* 50:1001–1011.

Sowemimo-Coker, S. O., P. Whittingstall, L. Pietsch, R. M. Bauersachs, R. B. Wenby, and H. J. Meiselman. 1989. Effects of cellular factors on the aggregation behavior of human, rat and bovine erythrocytes. *Clin. Hemorheol. Microcirc.* 9:723–737.

Tartakover-Matalon, S., H. Shoham-Kessary, V. Foltyn, and H. Gershon. 2000. Receptors involved in the phagocytosis of senescent and diamide-oxidized human RBCs. *Transfusion*. 40:1494–1502.

Vincent, B. 1990. The calculation of depletion layer thickness as a function of bulk polymer concentration. *Colloids and Surfaces*. 50:241–249.

Vincent, B., J. Edwards, S. Emmett, and A. Jones. 1986. Depletion flocculation in dispersions of sterically stabilised particles (''soft spheres''). *Colloids and Surfaces*. 18:261–281.

Walter, H., and K. E. Widen. 1994. Cell partitioning in two-polymer aqueous phase systems and cell electrophoresis in aqueous polymer solutions. Human and rat young and old red blood cells. *Biochim. Biophys. Acta*. 1194:131–137.

Whittingstall, P., and H. J. Meiselman. 1991. Effect of galactose incubation on the aggregation behavior of density-separated human erythrocytes. *In* Hemorheologie et Aggregation Erythrocytaire. J. F. Stoltz, M. Donner, and A. L. Copley, editors. Editions Medicales Internationales, Paris. 111–122.

Yaari, A. 1969. Mobility of human red blood cells of different age groups in an electric field. *Blood*. 33:159–163.